Diffusion-reaction model of positron annihilation for complex defect pattern

OPEN ACCESS
IOP Publishing
Journal of Physics: Condensed Matter
J. Phys.: Condens. Matter **36** (2024) 125703 (9pp)
https://doi.org/10.1088/1361-648X/ad1279

Diffusion-reaction model of positron annihilation for complex defect pattern

Philipp Brunner and Roland Würschum*

Institute of Materials Physics, Graz University of Technology, NAWI Graz, Petersgasse 16, Graz A-8010, Austria

E-mail: wuerschum@tugraz.at

Received 28 August 2023, revised 21 November 2023
Accepted for publication 5 December 2023
Published 15 December 2023

Abstract

The increasing structural complexity in modern material science is often associated with grain sizes in the μm- and the sub-μm-regime. Therefore, when positron annihilation is applied for studying free-volume type defects in such materials, positron trapping at grain boundaries (GBs) cannot be neglected, even when other defect types are in the primary focus. For this purpose, the available diffusion-reaction model for positron trapping and annihilation at GBs is extended to competitive trapping at two different types of intragranular defects. Closed-form expressions for the mean positron lifetime and the relative intensities of the defect-specific positron lifetime components are given. The model is presented for cylindrical-shaped crystallites, but is valid in the general sense for spherical symmetry as well with appropriate replacements. The model yields the basis for properly determining defect concentrations, even for the inconvenient but common case that one intragranular defect type exhibits a lifetime component similar to that in GBs. It turns out, that positron trapping at GBs matters even for μm-sized crystallites and should not be neglected for precise studies of intragranular defects.

Keywords: positron annihilation, diffusion-reaction model, defects, grain boundaries, interfaces

1. Introduction

Positron annihilation represents a well-established and sensitive probe technique for the study of atomic-scale sized free volumes in condensed matter [1–3]. In the classical former field of point-defect studies in coarse-grained metals, positron (e^+) trapping at grain boundaries (GBs) could be safely set aside. The increasing structural complexity in modern material science is, however, often associated with grain sizes in the μm- and the sub-μm-regime. In these application fields of positron annihilation, e^+-trapping at GBs can no longer be neglected, even when other defect types, rather than GBs, are in the primary focus of study.

For this purpose, a model for e^+-trapping and annihilation both in GBs and two different types of intragranular defects is presented in this paper. Such complex defect scenarious may prevail, e.g. in metals after strong plastic deformation [4–7] or else in corroded [8] or hydrogen-loaded fine-grained metals [9, 10], where in addition to GBs, dislocations and voids may act as positron trap. Another example are porous metals with a high-fraction of interfaces, lattice vacancies and voids [11–13]. Although three different defect-associated positron lifetimes may in practice hardly be distinguishable, the model is of high relevance in the inconvenient but common case that one intragranular defect type (e.g. vacancy or dislocation) exhibits a lifetime component similar to that in GBs. The error in determining the concentration of this type of intragranular defect is critically assessed when in such a case, positron trapping at GBs is not taken into account.

* Author to whom any correspondence should be addressed.

As outlined and worked out earlier, e^+ trapping at GBs has to be treated in the framework of diffusion-reaction models in order to take the diffusion-limitation in the trapping process properly into consideration [6, 14–20]. The mathematical approach [15], which is used here, as well as by another group [16], has the attractive feature that it yields closed-form expressions of the major e^+ annihilation parameters. This enables direct insight in the physical details of e^+ annihilation characteristics as well as a convenient application for the analysis of experimental data.

A quantitative analysis of the present model with characteristic data sets leads to the conclusion that positron trapping at GBs matters even for μm-sized crystallites and should not be neglected for precise studies of intragranular defects. From this point of view, the present work is of general relevance for positron annihilation studies of polycrystalline materials.

2. The model

The model describes the positron annihilation characteristics in polycrystalline materials where positrons are trapped and annihilated both in defects inside the grains and free-volume type defects in GBs. Extending the available models for spherical-shaped grains with a single type of point defect inside the grains [6, 16, 17], the present model considers two different types of intragranular defects with concentrations C_i $(i = 1,2)$ and crystallites with cylindrical shape of infinite length. Trapping at the intergranular defects is handled by standard rate theory, whereas for e^+ trapping at GBs both the e^+ diffusion and the transition reaction at the grain boundary is taken into account (so called diffusion-reaction controlled trapping process). Although for the sake of conciseness, the calculation is done for cylindrical symmetry, with appropriate replacements the model results are valid for spherical symmetry as well (see section 2.5). The model results for both geometries will be compared with each other (see section 3)

The behavior of the positrons is described by their bulk (free) lifetime τ_f, by their characteristic lifetimes $(\tau_i, i = 1,2)$ in the two types of intragranular defects, by their lifetime (τ_b) in the GBs, and by their bulk diffusivity D. Trapping at the intragranular defects and the grain boundary are characterized by the specific e^+ trapping rates σ_i $(i = 1,2)$ and α, respectively.

The temporal and spatial evolution of the density ρ_g of free positrons within the grains is given by:

$$\frac{\partial \rho_g}{\partial t} = D\nabla^2 \rho_g - \rho_g \left(\tau_f^{-1} + \sigma_1 C_1 + \sigma_2 C_2\right) \tag{1}$$

where C_i denotes the concentrations of intragranular defects. The e^+ trapped in GBs of cylindrical-shaped crystallites (radius r_0) are described by the area density, ρ_b, i.e. the number of e^+ per GB unit area, for which the rate equation

$$\frac{\mathrm{d}\rho_b}{\mathrm{d}t} = \alpha \rho_g (r_0, t) - \tau_b^{-1} \rho_b \tag{2}$$

holds. The temporal evolution of the number of e^+ trapped in the two types of intragranular defects is given by

$$\frac{\mathrm{d}N_i}{\mathrm{d}t} = -\tau_i^{-1} N_i + \sigma_i C_i N_f \tag{3}$$

where the number N_f of positrons in the free state follows from integration of ρ_g over the crystallite volume

$$N_f = \int \rho_g \mathrm{d}V. \tag{4}$$

Note that detrapping of e^+ from the intragranular defects or from the GB trapped state is not considered. The continuity of the e^+ flux at the grain boundary defines the boundary condition:

$$D\nabla \rho_g \Big|_{r=r_0} + \alpha \rho_g (r_0, t) = 0. \tag{5}$$

As initial condition, it is as usually assumed that positrons are exclusively in the free state, homogeneously distributed in the grains with initial density $\rho_g = \rho_g(0)$. This is well justified since the GB volume can be neglected with respect to the crystallite volume. The grain boundary is therefore considered as strictly two-dimensional in the present model.

Following the earlier works [15–17], the time dependence is handled by the Laplace transforms

$$\tilde{\rho}_{g,b}(r,p) = \int_0^\infty \exp(-pt)\, \rho_{g,b}(\mathbf{r},t)\, \mathrm{d}t, \tag{6a}$$

$$\tilde{N}_{i,f}(p) = \int_0^\infty \exp(-pt)\, N_{i,f}(t)\, \mathrm{d}t, \tag{6b}$$

which leads to the basic equations for this diffusion-reaction model with cylindrical symmetry

$$\frac{\mathrm{d}^2 \tilde{\rho}_g}{\mathrm{d}r^2} + \frac{1}{r}\frac{\mathrm{d}\tilde{\rho}_g}{\mathrm{d}r} - \gamma^2 \tilde{\rho}_g = -\frac{\rho_g(0)}{D} \tag{7a}$$

with

$$\gamma^2 = \gamma^2(p) := \frac{\tau_f^{-1} + \sigma_1 C_1 + \sigma_2 C_2 + p}{D} \tag{7b}$$

and

$$\tilde{\rho}_b = \frac{\alpha \tilde{\rho}_g (r_0, p)}{\tau_b^{-1} + p}, \tag{7c}$$

$$\tilde{N}_i = \frac{\sigma_i C_i}{\tau_i^{-1} + p} \tilde{N}_f, \tag{7d}$$

$(i = 1,2)$ with the boundary condition

$$D \frac{\mathrm{d}\tilde{\rho}_g}{\mathrm{d}r}\Big|_{r=r_0} + \alpha \tilde{\rho}_g (r_0, p) = 0. \tag{7e}$$

The solution of the differential equation (7*a*) satisfying equation (7*e*) can be written as

$$\tilde{\rho}_g(r,p) = A I_0(\gamma r) + \frac{\rho_g(0)}{\tau_f^{-1} + \sigma_1 C_1 + \sigma_2 C_2 + p}, \tag{8}$$

$$A = \frac{-\alpha \rho_g(0)}{\left(\tau_f^{-1} + \sigma_1 C_1 + \sigma_2 C_2 + p\right)\left[D\gamma I_1(\gamma r_0) + \alpha I_0(\gamma r_0)\right]} \tag{9}$$

with $I_0(\gamma r_0)$ and $I_1(\gamma r_0)$ as the modified Bessel functions.

For analysis of positron annihilation experiments of relevance is the total probability $n(t)$ that a e^+ implanted at $t = 0$ has not yet been annihilated at time t. $n(t)$ is given by the fraction of e^+ per unit length of cylinder at time t:

$$n(t) = \frac{1}{\pi r_0^2 \rho_g(0)} \left\{ \int_0^{r_0} 2\pi r \rho_g(\mathbf{r},t)\,\mathrm{d}r + 2\pi r_0 \rho_b(t) + N_1(t) + N_2(t) \right\}. \tag{10}$$

Taking into account the solutions of $\tilde{N}_i$ (equation (7*d*)), the Laplace transform of $n(t)$ reads

$$\tilde{n}(p) = \frac{1}{\pi r_0^2 \rho_g(0)} \left\{ \left(1 + \frac{\sigma_1 C_1}{\tau_1^{-1} + p} + \frac{\sigma_2 C_2}{\tau_2^{-1} + p}\right) \times \int_0^{r_0} 2\pi r \tilde{\rho}_g(\mathbf{r},p)\,\mathrm{d}r + 2\pi r_0 \tilde{\rho}_b(t) \right\}. \tag{11}$$

Solving the integral $\left(\int_0^{r_0} r I_0(\gamma r)\mathrm{d}r = (r_0/\gamma) I_1(\gamma r_0)\right)$ for the solution of the differential equation (8) and inserting $\tilde{\rho}_b(p)$ (equation (7*c*)) yields:

$$\begin{aligned}\tilde{n}(p) = {} & \left\{ \frac{2\alpha}{r_0} \gamma D \Theta(\gamma r_0) \left[\sigma_1 C_1 \left(\tau_2^{-1} + p\right)\left(\tau_1^{-1} - \tau_b^{-1}\right) \right.\right. \\ & + \sigma_2 C_2 \left(\tau_1^{-1} + p\right)\left(\tau_2^{-1} - \tau_b^{-1}\right) \\ & \left. + \left(\tau_1^{-1} + p\right)\left(\tau_2^{-1} + p\right)\left(\tau_f^{-1} - \tau_b^{-1}\right) \right] + \left[\alpha + \gamma D \Theta(\gamma r_0)\right] \\ & \times \left(\tau_b^{-1} + p\right)\left(\tau_f^{-1} + \sigma_1 C_1 + \sigma_2 C_2 + p\right) \left[\sigma_1 C_1 \left(\tau_2^{-1} + p\right) \right. \\ & \left.\left. + \sigma_2 C_2 \left(\tau_1^{-1} + p\right) + \left(\tau_1^{-1} + p\right)\left(\tau_2^{-1} + p\right) \right] \right\} \\ & \times \left\{ \left[\alpha + \gamma D \Theta(\gamma r_0)\right]\left(\tau_1^{-1} + p\right)\left(\tau_2^{-1} + p\right) \right. \\ & \left. \times \left(\tau_b^{-1} + p\right)\left(\tau_f^{-1} + \sigma_1 C_1 + \sigma_2 C_2 + p\right)^2 \right\}^{-1}\end{aligned} \tag{12}$$

with

$$\Theta(z) = \frac{I_1(z)}{I_0(z)}. \tag{13}$$

For a single type of intragranular defect, i.e. $C_2 = 0$, $\tilde{n}(p)$ simplifies to

$$\begin{aligned}\tilde{n}(p) = {} & \left\{ \frac{2\alpha}{r_0} \gamma D \Theta(\gamma r_0) \left[\sigma_1 C_1 \left(\tau_1^{-1} - \tau_b^{-1}\right) \right.\right. \\ & \left. + \left(\tau_1^{-1} + p\right)\left(\tau_f^{-1} - \tau_b^{-1}\right) \right] \\ & + \left[\alpha + \gamma D \Theta(\gamma r_0)\right]\left(\tau_b^{-1} + p\right) \\ & \times \left(\tau_f^{-1} + \sigma_1 C_1 + p\right)\left[\sigma_1 C_1 + \left(\tau_1^{-1} + p\right)\right] \Big\} \\ & \times \left\{ \left[\alpha + \gamma D \Theta(\gamma r_0)\right]\left(\tau_1^{-1} + p\right) \right. \\ & \left. \times \left(\tau_b^{-1} + p\right)\left(\tau_f^{-1} + \sigma_1 C_1 + p\right)^2 \right\}^{-1}.\end{aligned} \tag{14}$$

The Laplace transform $\tilde{n}(p)$ (equation (12)) represents the entire solution of the present diffusion and trapping model from which both the mean positron lifetime and the positron lifetime spectrum can be deduced. In the following, the solutions for the general case (section 2.1), for exclusive grain boundary trapping (section 2.2), for the limiting case of reaction-controlled GB trapping (section 2.3) as well as approximate solutions for minor diffusion limitation (section 2.4) will be presented. In addition, the corresponding solutions for spherical symmetry will be shortly addressed (section 2.5).

2.1. General solution

The mean positron lifetime $\overline{\tau}$ is obtained by taking the Laplace transform at $p = 0$:

$$\begin{aligned}\overline{\tau} = \tilde{n}(p=0) = {} & \left\{ \frac{2\alpha}{r_0} \gamma_0 D \Theta(\gamma_0 r_0) \right. \\ & \times \left[\tau_b \left(\tau_f^{-1} + \sigma_1 C_1 + \sigma_2 C_2\right) - \left(1 + \sigma_1 C_1 \tau_1 + \sigma_2 C_2 \tau_2\right) \right] \\ & + \left[\alpha + \gamma_0 D \Theta(\gamma_0 r_0)\right]\left(\tau_f^{-1} + \sigma_1 C_1 + \sigma_2 C_2\right) \\ & \left. \times \left(1 + \sigma_1 C_1 \tau_1 + \sigma_2 C_2 \tau_2\right) \right\} \\ & \times \left\{ \left[\alpha + \gamma_0 D \Theta(\gamma_0 r_0)\right]\left(\tau_f^{-1} + \sigma_1 C_1 + \sigma_2 C_2\right)^2 \right\}^{-1}\end{aligned} \tag{15}$$

with

$$\gamma_0 = \sqrt{\frac{\tau_f^{-1} + \sigma_1 C_1 + \sigma_2 C_2}{D}}. \tag{16}$$

The positron lifetime spectrum follows from $\tilde{n}(p)$ (equation (12)) by means of Laplace inversion. The single poles p of $\tilde{n}(p)$ yield the characteristic annihilation rates, i.e. the inverse of the positron lifetime components; their relative intensities is given by the residues of $\tilde{n}(p)$.

The intensity of the grain-boundary trapped state with the characteristic annihilation rate τ_b^{-1} (pole $p = -\tau_b^{-1}$) reads

$$I_b = \frac{2\alpha}{r_0}\frac{\gamma_b D\Theta(\gamma_b r_0)}{[\alpha+\gamma_b D\Theta(\gamma_b r_0)]\left(\tau_f^{-1}+\sigma_1 C_1+\sigma_2 C_2-\tau_b^{-1}\right)} \quad (17a)$$

or

$$I_b = \frac{2\alpha}{r_0}\frac{\Theta(\gamma_b r_0)}{\gamma_b[\alpha+\gamma_b D\Theta(\gamma_b r_0)]} \quad (17b)$$

with

$$\gamma_b = \sqrt{\frac{\tau_f^{-1}+\sigma_1 C_1+\sigma_2 C_2-\tau_b^{-1}}{D}}. \quad (18)$$

The characteristic annihilation rates τ_i^{-1} (poles $p=-\tau_i^{-1}$, $i=1,2$) of the intragranular-trapped states are associated with the intensities

$$I_i = \sigma_i C_i \frac{[\alpha+\gamma_i D\Theta(\gamma_i r_0)]\left(\tau_f^{-1}+\sigma_1 C_1+\sigma_2 C_2-\tau_i^{-1}\right)-\frac{2\alpha}{r_0}\gamma_i D\Theta(\gamma_i r_0)}{[\alpha+\gamma_i D\Theta(\gamma_i r_0)]\left(\tau_f^{-1}+\sigma_1 C_1+\sigma_2 C_2-\tau_i^{-1}\right)^2} \quad (19)$$

with

$$\gamma_i = \sqrt{\frac{\tau_f^{-1}+\sigma_1 C_1+\sigma_2 C_2-\tau_i^{-1}}{D}}. \quad (20)$$

The poles of $\tilde{n}(p)$ (equation (12)) defined by $\alpha+\gamma D\Theta(\gamma r_0)=0$ are given by the real positive solutions of

$$x\frac{J_1(x)}{J_0(x)} = \frac{\alpha r_0}{D} \quad (21)$$

($J_1(x), J_0(x)$: Bessel functions of first kind) with $x=\gamma_{j,0}^{\star} r_0$, where $\gamma_{j,0}^{\star}$ is associated with the characteristic annihilation rates $\lambda_{0,j}$ as follows:

$$\gamma_{0,j}^{\star} = \sqrt{\frac{\lambda_{0,j}-\left(\tau_f^{-1}+\sigma_1 C_1+\sigma_2 C_2\right)}{D}}, \quad (22)$$

where the index j enumerates the roots of equation (21). Equation (21) is based on the relation $\gamma I_1(\gamma r_0)/I_0(\gamma r_0) = -\gamma^{\star} J_1(\gamma^{\star} r_0)/J_0(\gamma^{\star} r_0)$ with $\gamma^{\star}=i\gamma$. This transcendental equation has the typical form for this type of reaction-controlled boundary condition with cylindrical symmetry [21]. From the residues the associated intensities

$$\begin{aligned} I_{0,j} = \frac{4\alpha}{r_0}\Big[&\sigma_1 C_1\left(\tau_2^{-1}-\lambda_{0,j}\right)\left(\tau_1^{-1}-\tau_b^{-1}\right) \\ &+\sigma_2 C_2\left(\tau_1^{-1}-\lambda_{0,j}\right)\left(\tau_2^{-1}-\tau_b^{-1}\right) \\ &+\left(\tau_1^{-1}-\lambda_{0,j}\right)\left(\tau_2^{-1}-\lambda_{0,j}\right)\left(\tau_f^{-1}-\tau_b^{-1}\right)\Big] \\ &\times\left\{\left[\frac{\alpha r_0}{D}-\frac{r_0}{\alpha}\left(\tau_f^{-1}+\sigma_1 C_1+\sigma_2 C_2-\lambda_{0,j}\right)\right]\right. \\ &\times\left(\tau_1^{-1}-\lambda_{0,j}\right)\left(\tau_2^{-1}-\lambda_{0,j}\right)\left(\tau_b^{-1}-\lambda_{0,j}\right) \\ &\left.\times\left(\tau_f^{-1}+\sigma_1 C_1+\sigma_2 C_2-\lambda_{0,j}\right)\right\}^{-1} \end{aligned} \quad (23)$$

are obtained.

The second-order pole of $\tilde{n}(p)$ (equation (12)) at $p=-(\tau_f^{-1}+\sigma_1 C_1+\sigma_2 C_2)$ yields no contribution. Closer inspection by means of series expansion of $\Theta(z)$ shows that the intensity associated with this pole cancels. Therefore, in summary the e^+ lifetime spectrum reads

$$\begin{aligned} n(t) = I_1\exp\left(-\frac{t}{\tau_1}\right)+I_2\exp\left(-\frac{t}{\tau_2}\right)+I_b\exp\left(-\frac{t}{\tau_b}\right) \\ +\sum_{j=1}^{\infty} I_{0,j}\exp(-\lambda_{0,j}t). \end{aligned} \quad (24)$$

The sequence of annihilation rates $\lambda_{0,j} > \tau_f^{-1}$ characterizes the rates by which positrons are removed from the free state. In practice, only one or a few components of the sequence are of relevance (see section 3).

The analogous extension of the above equations to more than two types of intragranular defects is straightforward, but of less relevance due to the limited number of e^+ lifetime components, that can in practice be resolved.

2.2. Special case of exclusive grain boundary trapping

For negligible trapping inside the grains, i.e. $\sigma_i C_i \ll \tau_f^{-1}$ ($i=1,2$) the model contains as limiting case the solutions of the diffusion-reaction model for positron trapping exclusively in GBs of cylindrical-shaped crystallites. The Laplace transform $\tilde{n}(p)$ (equation (12)) becomes

$$\begin{aligned} \tilde{n}(p) = &\left\{\frac{2\alpha}{r_0}\gamma D\Theta(\gamma r_0)\left(\tau_f^{-1}-\tau_b^{-1}\right)\right. \\ &\left.+[\alpha+\gamma D\Theta(\gamma r_0)]\left(\tau_f^{-1}+p\right)\right\} \\ &\times\left\{[\alpha+\gamma D\Theta(\gamma r_0)]\left(\tau_b^{-1}+p\right)\left(\tau_f^{-1}+p\right)^2\right\}^{-1}, \end{aligned} \quad (25)$$

the mean positron lifetime (compare equation (15))

$$\overline{\tau} = \tau_f \frac{\frac{2\alpha}{r_0}\gamma_0 D\,\Theta(\gamma_0 r_0)(\tau_b - \tau_f) + \alpha + \gamma_0 D\,\Theta(\gamma_0 r_0)}{\alpha + \gamma_0 D\,\Theta(\gamma_0 r_0)}, \quad (26)$$

the intensity of the GB annihilation component τ_b^{-1} as given by equation (17*b*), and the intensities of the rate constants $\lambda_{0,j}$ (compare equation (23))

$$I_{0,j} = \frac{\frac{4\alpha}{r_0}\left(\tau_f^{-1} - \tau_b^{-1}\right)}{\left[\frac{\alpha r_0}{D} - \frac{r_0}{\alpha}\left(\tau_f^{-1} - \lambda_{0,j}\right)\right]\left(\tau_f^{-1} - \lambda_{0,j}\right)\left(\tau_b^{-1} - \lambda_{0,j}\right)} \quad (27)$$

with γ_0 (equation (16)), γ_b (equation (18)), and $\gamma_{0,j}^{\star}$ (equation (22)) for $C_1 = C_2 = 0$.

The cylinder-symmetrical case without intragranular defects has been calculated by Dryzek *et al* [16], earlier. The solutions I_b (equation (17*b*)) and $I_{0,j}$ (equation (27)) are identical to those in [16].

2.3. Limiting case of reaction-controlled GB trapping

For the sake of completeness, it is shown in the following that the present diffusion-reaction model contains as special case of high e^+ diffusivity and/or small grain size the standard reaction model. For $\gamma r_0 \ll 1$, the function Θ (equation (13)) can be expanded. Restriction to first order ($\Theta(z) = z/2$) yields

$$\gamma D\,\Theta(\gamma r_0) = \frac{r_0}{2}\left(\tau_f^{-1} + \sigma_1 C_1 + \sigma_2 C_2 + p\right) \quad (28)$$

for which the Laplace transform (equation (12)) becomes independent of the diffusivity D:

$$\begin{aligned}\tilde{n} = \Bigg\{ & \frac{2\alpha}{r_0}\left(\tau_1^{-1} + p\right)\left(\tau_2^{-1} + p\right) + \left(\tau_b^{-1} + p\right) \\ & \times \Big[\sigma_1 C_1\left(\tau_2^{-1} + p\right) + \sigma_2 C_2\left(\tau_1^{-1} + p\right) \\ & + \left(\tau_1^{-1} + p\right)\left(\tau_2^{-1} + p\right)\Big]\Bigg\} \\ & \times \Bigg\{\left(\tau_f^{-1} + \frac{2\alpha}{r_0} + \sigma_1 C_1 + \sigma_2 C_2 + p\right) \\ & \times \left(\tau_1^{-1} + p\right)\left(\tau_2^{-1} + p\right)\left(\tau_b^{-1} + p\right)\Bigg\}^{-1}. \end{aligned} \quad (29)$$

By means of Laplace inversion of equation (29) the well-known solution of the simple trapping model for three types of e^+ traps [22, 23] is recovered. From the poles of equation (29), the e^+ annihilation rates in the intragranular defect trapped states (τ_i^{-1}, $i = 1,2$) and grain-boundary trapped state (τ_b^{-1}), and, in addition, the rate constant

$$\frac{1}{\tau_0} = \frac{1}{\tau_f} + \frac{2\alpha}{r_0} + \sigma_1 C_1 + \sigma_2 C_2 \quad (30)$$

follows. The rate τ_0^{-1}, by which e^+ are removed from the free state, is given by the sum of the free e^+ annihilation rate τ_f^{-1} and the trapping rates $2\alpha r_0^{-1}$ and $\sigma_i C_i$ ($i = 1,2$) of GBs and intragranular defects, respectively. Calculation of the residues yields the corresponding relative intensities

$$I_b = \frac{\frac{2\alpha}{r_0}}{\tau_f^{-1} + \frac{2\alpha}{r_0} + \sigma_1 C_1 + \sigma_2 C_2 - \tau_b^{-1}}, \quad (31a)$$

$$I_i = \frac{\sigma_i C_i}{\tau_f^{-1} + \frac{2\alpha}{r_0} + \sigma_1 C_1 + \sigma_2 C_2 - \tau_i^{-1}}, \quad (31b)$$

($i = 1,2$),

$$I_0 = 1 - I_b - I_1 - I_2. \quad (31c)$$

With $\tilde{n}(p)$ (equation (29)) for $p = 0$ the mean positron lifetime reads

$$\overline{\tau} = \tau_f \frac{1 + \frac{2\alpha}{r_0}\tau_b + \sigma_1 C_1 \tau_1 + \sigma_2 C_2 \tau_2}{1 + \frac{2\alpha}{r_0}\tau_f + \sigma_1 C_1 \tau_f + \sigma_2 C_2 \tau_f}. \quad (32)$$

2.4. Approximate solution for minor diffusion limitation

Approximate solutions for minor diffusion limitation follow from expansion of $\Theta(z)$ (equation (13)) up to third order: $\Theta(z) = z/2 - z^3/16$. Applying this expansion for I_b (equation (17*a*)) yields

$$I_b = \frac{2\alpha}{r_0} \frac{1 - \frac{r_0^2}{8D}\left(\tau_f^{-1} + \sigma_1 C_1 + \sigma_2 C_2 - \tau_b^{-1}\right)}{\tau_f^{-1} + \frac{2\alpha}{r_0} + \sigma_1 C_1 + \sigma_2 C_2 - \tau_b^{-1} - \frac{r_0^2}{8D}\left(\tau_f^{-1} + \sigma_1 C_1 + \sigma_2 C_2 - \tau_b^{-1}\right)^2}, \quad (33)$$

correspondingly for I_i (equation (19))

$$I_i = \sigma_i C_i \frac{1 - \frac{r_0^2}{8D}\left(\tau_f^{-1} + \sigma_1 C_1 + \sigma_2 C_2 - \tau_i^{-1} - \frac{2\alpha}{r_0}\right)}{\tau_f^{-1} + \frac{2\alpha}{r_0} + \sigma_1 C_1 + \sigma_2 C_2 - \tau_i^{-1} - \frac{r_0^2}{8D}\left(\tau_f^{-1} + \sigma_1 C_1 + \sigma_2 C_2 - \tau_i^{-1}\right)^2}, \tag{34}$$

($i = 1,2$) and for $\overline{\tau}$ (equation (15))

$$\begin{aligned}\overline{\tau} = \tau_f \Bigg\{ & 1 + \frac{2\alpha}{r_0}\tau_b + \sigma_1 C_1 \tau_1 + \sigma_2 C_2 \tau_2 - \frac{r_0^2}{8D} \\ & \times \left[\left(1 + \frac{2\alpha}{r_0}\tau_b + \sigma_1 C_1 \tau_1 + \sigma_2 C_2 \tau_2\right)\left(\tau_f^{-1} + \sigma_1 C_1 + \sigma_2 C_2\right) \right. \\ & \left. - \frac{2\alpha}{r_0}\left(1 + \sigma_1 C_1 \tau_1 + \sigma_2 C_2 \tau_2\right) \right] \Bigg\} \\ & \times \Bigg\{ 1 + \frac{2\alpha}{r_0}\tau_f + \sigma_1 C_1 \tau_f + \sigma_2 C_2 \tau_f \\ & - \frac{r_0^2}{8D}\tau_f\left(\tau_f^{-1} + \sigma_1 C_1 + \sigma_2 C_2\right)^2 \Bigg\}^{-1}. \end{aligned} \tag{35}$$

These equations contain in the limit of high diffusivity and/or small grain size, i.e. when the summands $r_0^2/(8D)(\tau_f^{-1} + \ldots)$ become negligible, the standard solutions of rate theory (equations (31*a*), (31*b*) and (32)).

2.5. Spherical symmetry

The diffusion-reaction model for spherical-shaped grains with a single type of point defect inside the spherical-shaped grains has been elaborated earlier [16, 17]. Without proof, we note that the present solutions $\tilde{n}(p)$ (equation (12)), $\overline{\tau}$ (equation (15)), I_b (equation (17*b*)), and I_i (equation (19)) for two types of intragranular traps ($i = 1,2$) with cylindrical-shaped crystallites are valid in the general sense also for the spherical symmetry, if in the present solutions $2/r_0$ is replaced by $3/r_0$ and $\Theta(z) = I_1(z)/I_0(z)$ by the Langevin function $L(z) = i_1(z)/i_0(z)$ (i_0, i_1: modified spherical Bessel functions). Indeed, with these replacements, the Laplace transform $\tilde{n}(p)$ for one type of intragranular trap given above (equation (14)) is identical to that given in [17] (equation (17) in [17]).

3. Discussion

We start the discussion with considering how the key parameters, i.e. the mean positron lifetime $\overline{\tau}$ and the relative intensities I_b, I_i ($i = 1,2$) of the defect-specific e^+-lifetime components depend on the crystallite size. Figure 1 shows the intensities I_b and I_i ($i = 1,2$) according to the general solution (equations (19) and (17*b*)) as a function of crystallite radius r_0; figure 2(among others) the corresponding r_0-variation of the mean positron lifetime $\overline{\tau}$ (equation (15)). The figures pertain to the practical relevant case that the e^+-lifetimes in the GB-trapped state and in the defect-trapped state of type 1 are the same, i.e., $\tau_b = \tau_1$, and of vacancy-type. Parameters τ_f, τ_b, τ_1, D, α, and σ_i typical for metals are used (see caption of figures 1 and 2, $D = 0.5 \times 10^{-4}$ m^{2}s^{-1} [24]; lattice vacancies $\sigma_1 = 4 \times 10^{14}$ s^{-1} [25]). For the second intragranular component, a lifetime $\tau_2 = 300$ ps as typical for small vacancy agglomerates is assumed. For the sake of illustration, concentrations $C_1 = C_2 = 10^{-5}$ of the two intragranular defect types are used which correspond to the center of the sensibility regime of the technique of positron annihilation.

Figure 1 shows that the intensity I_b of the GB-trapped state sigmoidally increases with decreasing crystallite radius, concomitantly the intensities I_i of the two intragranular trap components decreases. For small crystallite radii, GB trapping dominates, leading finally to the regime of saturation trapping at GBs ($I_b \to 1$). Apart from this saturation trapping regime, e^+-annihilation also occurs from the free, untrapped state as characterized by the sequence of decay rates $\lambda_{0,j} > \tau_f^{-1}$ (equation (24)). As typical for this kind of problems, the associated intensities $I_{0,j}$ (equation (23)) rapidly decrease and correspondingly the decay rates $\lambda_{0,j}$ (equation (22)) increase with increasing j, e.g. for $r_0 = 10^{-6}$ m with the parameter set according to figure 1: $I_{0,j=1} = 17.4\%$, $\lambda_{0,j=1} = 1/44$ ps^{-1}; $I_{0,j=2} = 2.9\%$, $\lambda_{0,j=2} = 1/42$ ps^{-1}; $I_{0,j=3} = 0.9\%$, $\lambda_{0,j=3} = 1/39$ ps^{-1}; $I_{0,j=4} = 0.4\%$, $\lambda_{0,j=4} = 1/35$ ps^{-1}. For selected r_0-values, the dominant first component $I_{0,j=1}$ is shown in figure 1; towards the regime of saturation trapping $I_{0,j=1}$ tends to 0.

As shown in figure 2, the mean positron lifetime $\overline{\tau}$ decreases with decreasing r_0 for the selected parameter set, since without or minor GB trapping $\overline{\tau}$ is enhanced to values above τ_b due to the proportionate trapping at the defect type 2 with longer component $\tau_2 = 300$ ps. For the purely reaction-controlled limit, the $\overline{\tau}$-curve is shifted to higher r_0-values, because in that case the limitation of trapping due to diffusion is neglected, i.e. the trapping at GBs is stronger. The approximation for minor diffusion-limitation describes the $\overline{\tau} - r_0$-variation very well in the regime of small r_0-values.

For comparison, also the case of exclusive grain boundary trapping (i.e. $C_1 = C_2 = 0$) is shown in figure 2, for diffusion-reaction limited trapping, for entirely reaction-controlled trapping, as well as for minor diffusion limitation. The mean e^+-lifetime shows the typical sigmoidal increase from τ_f to τ_b with decreasing crystallite size. For a given r_0-value, $\overline{\tau}$ is lower for diffusion-reaction limited trapping compared to purely reaction-controlled trapping because of diffusion limitation.

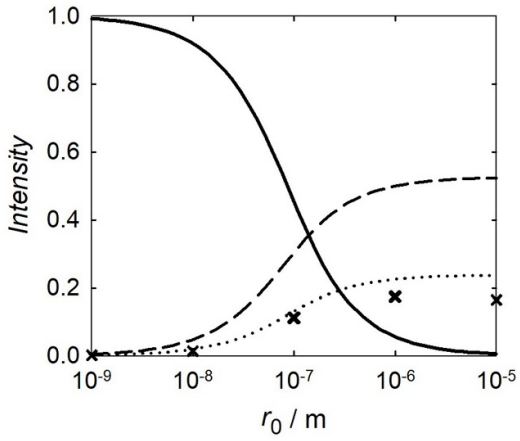

Figure 1. Intensities of GB component, I_b (equation (17*b*), solid line), and of two types of intragranular defects, I_1 (equation (19), $i = 1$, dotted line), I_2 (equation (19), $i = 2$, dashed line), as a function of radius r_0 of cylindrical-shaped grains. For selected r_0-values also the intensity $I_{0,j=1}$ of first component of the series $I_{0,j}$ (equation (23)) is shown (×). Parameters: $\tau_f = 120$ ps, $\tau_b = \tau_1 = 180$ ps, $\tau_2 = 300$ ps, $D = 0.5 \times 10^{-4}$ m^{2}s^{-1}, $\alpha = 10^3$ ms^{-1}, $\sigma_1 = 4 \times 10^{14}$ s^{-1}, $\sigma_2 = 10^{15}$ s^{-1}, $C_1 = C_2 = 10^{-5}$.

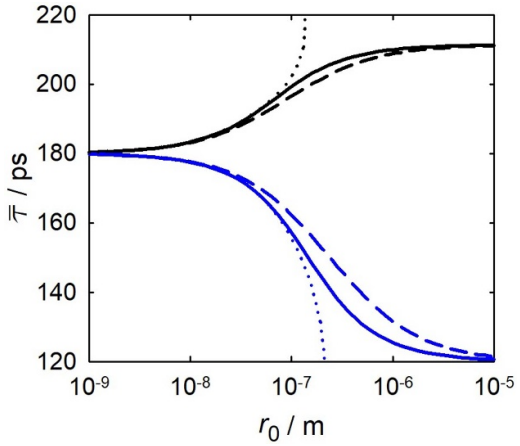

Figure 2. Mean positron lifetime $\overline{\tau}$ as a function of radius r_0 of cylindrical-shaped grains for exact solution (equation (15), black solid line), for limiting case of entirely reaction-controlled GB trapping (equation (32) black dashed line), and for approximate solution for minor diffusion limitation (equation (35), black dotted line) for the same parameter set as in figure 1. In addition both trapping models and the approximate solution for minor diffusion limitation are shown for exclusive grain boundary trapping (equation (26); equations (32) and (35) with $C_i = 0$, blue lines).

Again, the solution for minor diffusion-limitation is a good approximation in the regime of small r_0-values.

The figures 1 and 2 pertain to cylindrical-shaped crystallites. Figure 3 shows the comparison between cylindrical- and spherical-shaped crystallites for the intensity of the GB component, I_b, and the mean positron lifetime, $\overline{\tau}$, for the same parameter sets used in figures 1 and 2. Since the GB area related to the crystallite volume is higher for spherical-shaped crystallites than for cylindrical-shaped ones, meaning that the mean diffusion length to reach the GB is shorter, e^+-trapping at GBs for spherical is stronger than for cylindrical symmetry

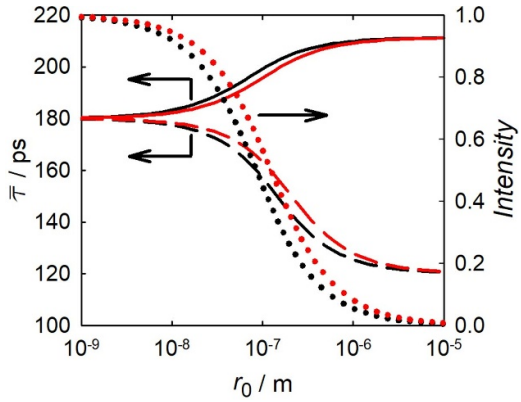

Figure 3. Intensity of GB component, I_b (dotted lines), and mean positron lifetime $\overline{\tau}$ (solid and dashed lines) as a function of radius r_0 of cylindrical-shaped grains (black) in comparison to spherical-shaped grains (red). The curves for the cylindrical symmetry are the same as shown in figure 1 (I_b) and in figure 2 ($\overline{\tau}$) for the exact solution. For the spherical symmetry the same parameter sets as quoted in the caption of figure 1 is used. The lower $\overline{\tau}$-curves (dashed lines) correspond to exclusive GB trapping (compare figure 2).

for the same crystallite size. Correspondingly, the variation of I_b and $\overline{\tau}$ with crystallite radius r_0 for spherical-shaped crystallites is shifted to higher r_0-values compared to cylindrical-shaped ones. The same conclusion has been drawn earlier by Dryzek and coworker [26], however, for a diffusion-reaction model where trapping at intergranular defects was not taken into account.

In the following we address the important issue that even for μm-sized crystallites e^+ trapping at GBs matters for correctly determining of concentrations of intragranular defects. From figure 1, already, it becomes clear that trapping at intragranular defects would be overestimated if e^+ trapping and annihilation at GBs is not taken into consideration, meaning that the intensity I_b due to GBs is added to that of the intragranular trap component (I_1). To visualize this quantitatively, figure 4 shows the supposed excess concentration ΔC_1 that arises when the sum $I_b + I_1$ of GB intensity and intragranular trap type 1 intensity is interpreted as arising from trap type 1, exclusively. It is evident, that in this way the trap concentration C_1 would be severely overestimated, with increasing trend for decreasing crystallite size. For spherical-shaped crystallites, this effect is even stronger than for cylindrical-shaped ones owing to the stronger GB trapping in the former case (compare red and black curves in figure 4).

The extent of overestimation depends on the characteristic parameters for GB trapping, i.e. on the e^+-diffusivity D and the specific trapping rate α. The figures shown above refer to typical parameter sets for D and α. Specific e^+ trapping rates α of GBs range from 200 ms^{-1} for Zn alloys to 3×10^3 ms^{-1} for Al alloys [14]. A substantially lower specific e^+ trapping rate $\alpha = 70$ ms^{-1} is reported for interfaces between matrix and semi-coherent precipitates [27]. To quantify the influence of α and D, table 1 shows the intensity of the GB component I_b (equation (17*b*)) for crystallites with a diameter ($2r_0$) of 10^{-6} m and various α-values, i.e. the maximum value of

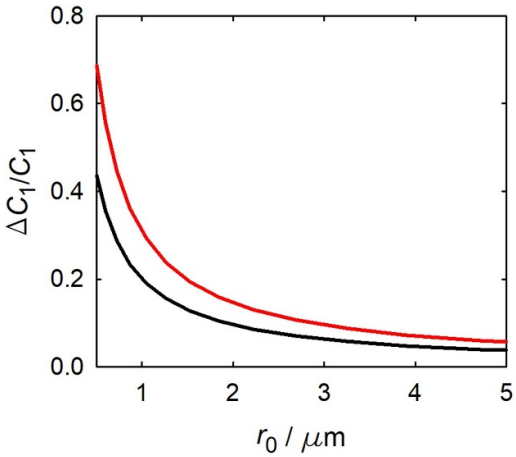

Figure 4. Relative deviation $\Delta C_1/C_1$ of intragranular defect concentration C_1 as a function of radius r_0, when e^+-trapping and annihilation in GB with identical e^+ lifetime ($\tau_1 = \tau_b$) is not taken into account. Black line for cylindrical-shaped grains, red line for spherical-shaped grains. Parameters: $\tau_f = 120$ ps, $\tau_b = \tau_1 = 180$ ps, $D = 0.5 \times 10^{-4}$ m^{2}s^{-1}, $\alpha = 10^3$ ms^{-1}, $\sigma_1 = 4 \times 10^{14}$ s^{-1}, $C_1 = 10^{-5}$, $C_2 = 0$. Deviation ΔC_1 is determined from $I_b + I_1 = \sigma_1(C_1 + \Delta C_1)[\tau_f^{-1} + \sigma_1(C_1 + \Delta C_1) - \tau_1^{-1}]^{-1}$ with exact solution of I_b (equation (17*b*)) and I_1 (equation (19)) for concentration C_1.

Table 1. Intensity I_b (equation (17*b*)) of GB component for exclusive GB trapping ($C_1 = 0$) at cylindrical shaped crystallites with radius $r_0 = 0.5$ μm and for the case of competitive trapping at intragranular defects with concentration C_1 and identical e^+ lifetime ($\tau_1 = \tau_b$) for selected values of e^+ diffusion coefficient D and specific GB trapping rate α. Parameters: $\tau_f = 120$ ps, $\tau_b = \tau_1 = 180$ ps, $\sigma_1 = 4 \times 10^{14}$ s^{-1}, $C_2 = 0$.

α [m s^{-1}]	3×10^3	10^3	70
D [m^{2}s^{-1}]		0.5×10^{-4}	
I_b ($C_1 = 0$)	0.41	0.35	0.083
I_b ($C_1 = 10^{-5}$)	0.27	0.20	0.036
D [m^{2}s^{-1}]		1×10^{-4}	
I_b ($C_1 = 0$)	0.52	0.42	0.086
I_b ($C_1 = 10^{-5}$)	0.34	0.25	0.038

3×10^3 ms^{-1} for GBs, the value of 70 ms^{-1} for semicoherent interfaces, and the value 10^3 ms^{-1} used in the figures considered characteristic for GBs. In addition to the D-value taken for the figures, the I_b-intensities are quoted for a value twice ($D = 10^{-4}$ m^{2}s^{-1}) as high.

The high I_b values show that substantial GB trapping occurs although the crystallite diameter of 1 μm by far exceeds the characteristic e^+ diffusion length $\sqrt{D\tau_f} \simeq 0.11$ μm (for $D = 10^{-4}$ m^{2}s^{-1} and $\tau_f = 120$ ps). Even for semicoherent interfaces with reduced α, GB trapping may not be neglected.

The GB trapping is still significant when competitive trapping at intragranular defects occurs as quoted in table 1 for a defect concentration C_1 of 10^{-5}, when the e^+-lifetimes in both trapped states are identical ($\tau_1 = \tau_b$). If in such a case one would not consider the e^+-trapping at GBs, quantitatively meaning that the GB component I_b is added to the intensity I_1 of the intragranular defect component (see caption figure 4), the concentration C_1 of this defect would be overestimated strongly, e.g. by $\Delta C_1 = 0.55 \times 10^{-5}$ or 0.44×10^{-5} for the examples $I_b = 0.25$ ($D = 10^{-4}$ m^{2}s^{-1}) or $I_b = 0.20$ ($D = 0.5 \times 10^{-4}$ m^{2}s^{-1}) of cylindrical-shaped crystallites given in table 1, i.e. the determined concentration would be 55% or 44% too high, respectively. For spherical-shaped crystallites, the overestimation would even be 87% or 69% for the same parameter set for $D = 10^{-4}$ m^{2}s^{-1} or 0.5×10^{-4} m^{2}s^{-1}, respectively.

In conclusion, e^+-trapping at GBs matters even for μm-sized crystallites and should not be neglected for precise studies of intragranular defects.

Data availability statement

All data that support the findings of this study are included within the article (and any supplementary files).

Authors contribution

Philipp Brunner: Formal analysis (supporting); Validation (equal); Visualization; Writing—original draft (supporting); Writing—review & editing (equal); **Roland Würschum:** Conceptualization; Formal analysis (lead); Validation (equal), Writing—original draft (lead); Writing—review & editing (equal).

ORCID iDs

Philipp Brunner https://orcid.org/0000-0003-2034-5762
Roland Würschum https://orcid.org/0000-0003-4624-4433

References

[1] Hautojärvi P 1979 *Positrons in Solids* (Springer)
[2] Hautojärvi P and Corbel C 1995 Positron spectroscopy of defects in metals and semiconductors *Positron Spectroscopy of Solids* (IOS Press) pp 491–532
[3] Krause-Rehberg R and Leipner H 1999 *Positron Annihilation in Semiconductors* (Springer)
[4] Würschum R, Greiner W, Valiev R, Rapp M, Sigle W, Schneeweiss O and Schaefer H E 1991 *Scr. Metall. Mater.* **25** 2451–6
[5] Würschum R, Kübler A, Gruß S, Scharwaechter P, Frank W, Valiev R, Mulyukov R and Schaefer H E 1996 *Ann. Chim.: Sci. Mater.* **21** 471–82
[6] Čížek J, Procházka I, Cieslar M, Kužel R, Kuriplach J, Chmelík F, Stulíková I, Bečvář F, Melikhova O and Islamgaliev R K 2002 *Phys. Rev.* B **65** 094106

[7] Čížek J 2018 *J. Mater. Sci. Technol.* **34** 577–98
[8] Brunner P, Brumbauer F, Steyskal E M, Renk O, Weinberg A M, Schroettner H and Würschum R 2021 *Biomater. Sci.* **9** 4099–109
[9] Krystian M, Setman D, Mingler B, Krexner G and Zehetbauer M 2010 *Scr. Mater.* **62** 49–52
[10] Edalati K, Akiba E and Horita Z 2018 *Sci. Technol. Adv. Mater.* **19** 185–93
[11] Viswanath R, Chirayath V, Rajaraman R, Amarendra G and Sundar C 2013 *Appl. Phys. Lett.* **102** 253101
[12] Rösner H, Parida S, Kramer D, Volkert C A and Weissmüller J 2007 *Adv. Eng. Mater.* **9** 535–41
[13] Erlebacher J 2011 *Phys. Rev. Lett.* **106** 225504
[14] Dupasquier A, Romero R and Somoza A 1993 *Phys. Rev.* B **48** 9235
[15] Würschum R and Seeger A 1996 *Phil. Mag.* **73** 1489–501
[16] Dryzek J, Czapla A and Kusior E 1998 *J. Phys.: Condens. Matter* **10** 10827
[17] Oberdorfer B and Würschum R 2009 *Phys. Rev.* B **79** 184103
[18] Würschum R, Resch L and Klinser G 2018 *Phys. Rev.* B **97** 224108
[19] Würschum R, Resch L and Klinser G 2019 *AIP Conf. Proc.* **2182** 050010
[20] Würschum R and Klinser G 2020 *Phil. Mag.* **100** 379–97
[21] Crank J 1979 *The Mathematics of Diffusion* 2nd edn (Oxford Science Publications)
[22] Connors D and West R 1969 *Phys. Lett.* **30** 24–25
[23] Frank W and Seeger A 1974 *Appl. Phys.* **3** 61–66
[24] Soininen E, Huomo H, Huttunen P, Mäkinen J, Vehanen A and Hautojärvi P 1990 *Phys. Rev.* B **41** 6227
[25] Schaefer H 1987 *Phys. Status Solidi* a **102** 47–65
[26] Dryzek J and Czapla A 1998 *J. Phys.: Condens. Matter* **10** L547
[27] Pahl W, Groger V, Krexner G and Dupasquier A 1995 *J. Phys.: Condens. Matter* **7** 5939